Real Space Imaging of Spin Polarons in Zn-Doped $SrCu_2(BO_3)_2$

M. Yoshida,[1] H. Kobayashi,[1] I. Yamauchi,[1] M. Takigawa,[1] S. Capponi,[2] D. Poilblanc,[2] F. Mila,[3] K. Kudo,[4] Y. Koike,[5] and N. Kobayashi[6]

[1]*Institute for Solid State Physics, University of Tokyo, Kashiwa, Chiba 277-8581, Japan*
[2]*Laboratoire de Physique Théorique, Université de Toulouse and CNRS, UPS (IRSAMC), F-31062 Toulouse, France*
[3]*Institut de Théorie des Phénomènes Physiques, École Polytechnique Fédérale de Lausanne, CH-1015 Lausanne, Switzerland*
[4]*Department of Physics, Okayama University, Okayama 700-8530, Japan*
[5]*Department of Applied Physics, Tohoku University, Sendai 980-8579, Japan*
[6]*Institute for Materials Research, Tohoku University, Sendai 980-8577, Japan*

(Received 23 July 2014; published 4 February 2015)

We report on the real space profile of spin polarons in the quasi-two-dimensional frustrated dimer spin system $SrCu_2(BO_3)_2$ doped with 0.16% of Zn. The ^{11}B nuclear magnetic resonance spectrum exhibits 15 additional boron sites near nonmagnetic Zn impurities. With the help of exact diagonalizations of finite clusters, we have deduced from the boron spectrum, the distribution of local magnetizations at the Cu sites with fine spatial resolution, providing direct evidence for an extended spin polaron. The results are confronted with those of other experiments performed on doped and undoped samples of $SrCu_2(BO_3)_2$.

DOI: 10.1103/PhysRevLett.114.056402 PACS numbers: 71.38.-k, 75.10.Jm, 75.25.-j, 76.60.Pc

Impurities and defects in strongly correlated quantum systems often produce significant effects over an extended spatial region, which can be studied by local probes such as nuclear or electron magnetic resonance (NMR or ESR) [1]. The best example is the edge states in Heisenberg spin chains. The spin 1/2 edge state in spin 1 Haldane chains is a direct consequence of the valence-bond-solid ground state of the pure system. The ESR experiments have played vital roles in identifying the edge spins [2,3] and their interactions [4]. The edge states are not localized at a single site but associated with local staggered magnetization due to the antiferromagnetic interaction of the bulk, and the spatial extent of such a polaronic structure is given by the correlation length of the bulk. The real space profile of spin polarons has been actually observed by NMR experiments in both spin 1 [5,6] and spin 1/2 [7] Heisenberg chains, from which the temperature dependence of the correlation length was deduced.

Although there have been less studies on two-dimensional (2D) systems, an interesting example is the frustrated 2D dimer spin system $SrCu_2(BO_3)_2$ with a small concentration of Cu^{2+} ions (spin 1/2) replaced by nonmagnetic Zn or Mg [8–11]. The magnetic layers contain orthogonal arrays of Cu dimers described by the Shastry-Sutherland lattice [12]

$$H = J\sum_{n.n.} \mathbf{S}_i \cdot \mathbf{S}_j + J'\sum_{n.n.n.} \mathbf{S}_i \cdot \mathbf{S}_j, \qquad (1)$$

where J (J') is the intradimer (interdimer) Heisenberg exchange interaction. The ground state of $SrCu_2(BO_3)_2$ at zero magnetic field is the dimer singlet state [13,14], which is known to be the exact ground state of Eq. (1) for $\alpha = J'/J$ not too large [12,15], less than $\alpha_c \simeq 0.675$ [16,17]. $SrCu_2(BO_3)_2$ exhibits a number of fascinating properties, most notably, a unique sequence of quantized magnetization plateaus in magnetic fields [18–23] which have been a subject of intense research in the last decade [24,25].

A nonmagnetic impurity creates an unpaired Cu^{2+} site in the dimer singlet state, producing a free spin 1/2. The structure factor of this spin 1/2 measured by inelastic neutron scattering experiments [10] points to an extended object. Theories have confirmed this picture and moreover, predicted the formation of a spin polaron extending over several sites around the impurity [9,11], clearly calling for further precise experimental information.

In this Letter, we report the observation of such a spin polaron in real space by ^{11}B NMR experiments on Zn-doped $SrCu_2(BO_3)_2$ performed in a sufficiently high magnetic field to saturate unpaired spins. With the help of exact diagonalization results, a nearly complete assignment of the 15 additional boron sites has been achieved, leading to the determination of the microscopic structure of a localized spin polaron with unprecedented accuracy.

Single crystals of $SrCu_{2-x}Zn_x(BO_3)_2$ were grown by the traveling-solvent floating-zone method [26,27]. Two crystals were used, $x = 0.0174$ and 0.0032 as determined by the inductively coupled plasma atomic emission spectrometry. The presence of free spins at low temperatures was confirmed by magnetization measurements (see Supplemental Material *A* [28]). The crystals were cut into a rod ($1 \times 1 \times 5$ mm^3) for NMR measurements, which were performed in a magnetic field B of 6.615 T precisely along the c axis (within ~0.2 degree).

The NMR spectra were obtained by summing the Fourier transform of the spin-echo signal obtained at equally spaced rf frequencies. Figure 1 shows the ^{11}B NMR spectrum for $x = 0.0032$ (0.16% of Zn) at 1.6 K. The

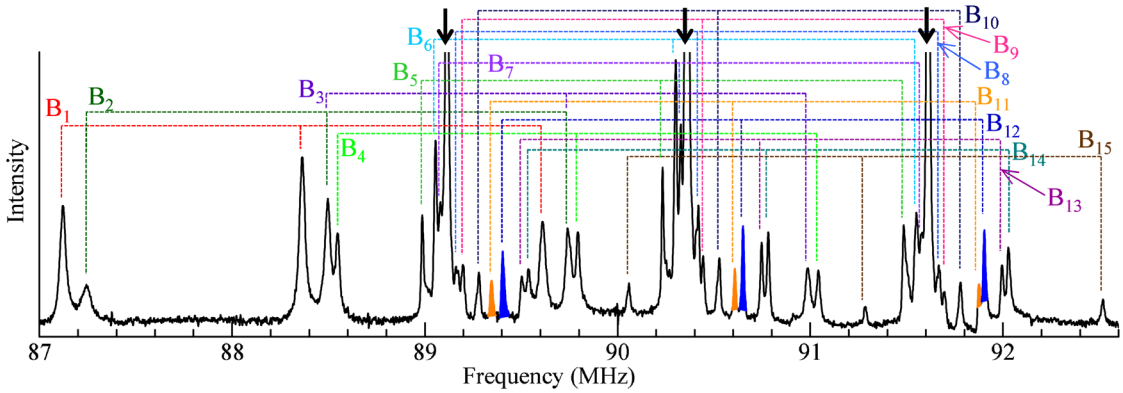

FIG. 1 (color online). ^{11}B NMR spectrum at $T = 1.6$ K and $B = 6.615$ T. The black arrows mark the position of the reference line (zero internal field). Fifteen additional lines named B_1 to B_{15} have been resolved. Note that B_1 is about twice as intense as B_2, and that B_{12} (shaded in blue) is also about twice as intense as B_{11} (shaded in orange).

Zeeman energy for the magnetic field of 6.615 T is much smaller than the zero-field energy gap for the triplet excitation in the bulk ($\Delta = 35$ K) but large enough to completely polarize the impurity induced free spins (see Supplemental Materials *A* and *B* [28]). To understand the ^{11}B NMR spectra, we first recall that one boron site generates three NMR lines at the frequencies $\nu_r = \gamma(B + B_{\rm int}) + k\nu_Q$, $(k = -1,\ 0,\ 1)$, where ν_Q is the quadrupole splitting along the c axis, $\gamma = 13.66$ MHz/T is the nuclear gyromagnetic ratio, and $B_{\rm int}$ is the internal magnetic field produced by nearby Cu spins. Since the Zn concentration is extremely dilute, most of Cu spins form singlet dimers generating $B_{\rm int} \sim 0$ at the majority of B sites. The NMR lines from these B sites (shown by black arrows) are very intense, far exceeding the range of display in Fig. 1.

In addition to this reference line, we have been able to identify 15 weaker lines with nonzero $B_{\rm int}$ (B_1–B_{15}, the thin lines in Fig. 1) and to determine the values of $B_{\rm int}$ and ν_Q for each of them. The sample with $x = 0.0174$ gives a nearly identical NMR spectrum (see Supplemental Material *C* [28]), ensuring no interference between impurities.

As we shall demonstrate, it is possible to assign most of the lines to specific boron sites and to deduce the polarization of the Cu sites around the impurity as shown in Fig. 2. To perform this line assignment, it is useful to know *a priori* the local magnetization expected in the neighborhood of a Zn impurity. We have thus performed exact diagonalizations (ED) calculation for finite-size clusters of the 2D Shastry-Sutherland lattice with 32 sites (31 spins and one vacancy) and 36 sites (35 spins and one vacancy), with periodic boundary conditions (see Supplemental Material *D* [28]). The ED results of Fig. 3(c) show that the local magnetization is distributed primarily over five spins surrounding the defect. A single spin at Cu_A with a large positive $\langle S_c^A \rangle \sim 0.18$–$0.30$, two spins at Cu_C with also a large positive $\langle S_c^C \rangle \sim 0.18$–$0.21$, and two spins at Cu_B with a large negative $\langle S_c^B \rangle \sim -0.1$ add up approximately to the saturated value of 0.5. In addition, eight spins at four other sites (Cu_{D-G}) carry a small and oscillating magnetization less than 0.1 in absolute value. The local magnetization is much smaller for the remaining sites ($\sim 10^{-3}$) and cannot be determined accurately for the cluster sizes of our calculation. Interestingly, there is a strong dependence on α. First of all, the polaronic structure collapses very rapidly when α exceeds 0.68, where the pure system undergoes a first-order transition from the dimer to the plaquette phase [16,17,32]. Besides, and more remarkably, the magnetization of the unpaired site Cu_A, $\langle S_c^A \rangle$, strongly depends on α.

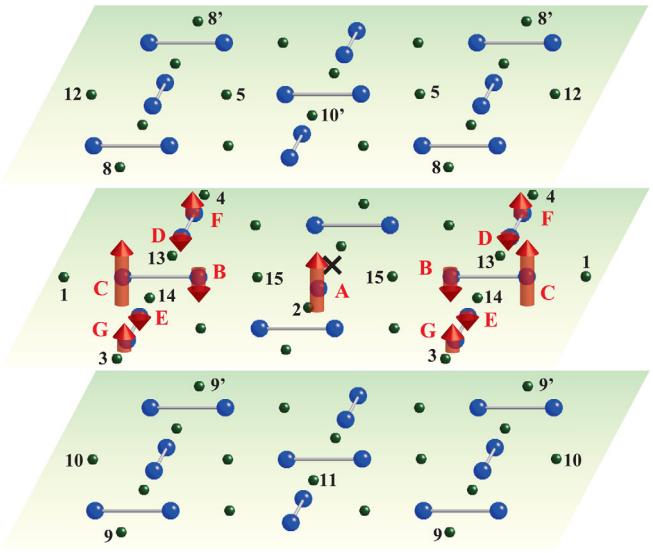

FIG. 2 (color online). Real space sketch of the spin polaron formed around a Zn impurity (cross). The up (down) arrows on the Cu sites represent the spin moments parallel (antiparallel) to the external field. The length of the arrow is proportional to $|\langle S_z \rangle|$ as calculated on a 36-site cluster with $J'/J = 0.67$. The numbers show the assignment of the B sites to the NMR lines of Fig. 1 deduced from the analysis described in the text. Primed numbers have been used when different sites are assigned to the same line. The other B sites have very small internal field.

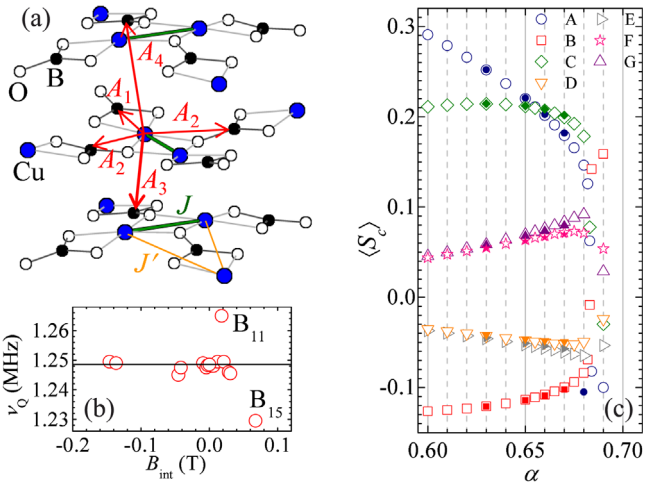

FIG. 3 (color online). (a) Main hyperfine couplings between a Cu spin and the B nuclei in the same layer (A_1 and A_2) or in the neighboring layers (A_3 or A_4). (b) Quadrupolar splitting ν_Q for B sites near a Zn impurity. (c) Dependence on $\alpha = J'/J$ of the local magnetization calculated with exact diagonalizations on a 32-site cluster (open symbols) and 36-site cluster (solid symbols).

It decreases steeply with α and becomes smaller than $\langle S_c^C \rangle$ at $\alpha \sim 0.66$, an observation that will turn crucial for the analysis of the experimental spectrum.

To make contact between the local magnetization at Cu sites and the boron spectrum, we note that the internal field $B_{\rm int}$ at a given boron site is given by the sum of contributions from neighboring Cu sites

$$B_{\rm int}^i = \sum_j A_{ij} \langle S_c^j \rangle. \quad (2)$$

Here, A_{ij} is the hyperfine coupling constant from the ith boron site to the jth Cu site. It is the sum of the dipolar and transferred hyperfine couplings, $A_{ij} = D_{ij} + T_{ij}$, and depends on the relative position between the boron and Cu sites. The dominant couplings are illustrated in Fig. 3(a) and summarized in Table I. The transferred hyperfine couplings are short ranged and limited to the nearest and next-nearest neighbors in the same layer, T_1 and T_2. They satisfy the condition $T_1 + 2T_2 = -0.431$ T imposed by the NMR shift data in undoped $SrCu_2(BO_3)_2$ [14], leaving only one adjustable parameter, say T_1. The analysis of NMR spectra in the magnetization plateau phases has led to the estimation $-0.71 < T_1 < -0.53$ T [22]. The dipolar

TABLE I. Hyperfine coupling constants in Tesla.

j	T_j	D_j	A_j
1	$-0.711 \sim -0.531$	-0.161	$-0.872 \sim -0.692$
2	$0.05 \sim 0.14$	-0.075	$-0.025 \sim 0.065$
3	0	0.103	0.103
4	0	0.065	0.065

couplings can be calculated from the crystal parameters. In addition to the nearest and next neareast neighbors in the same layer, two neighbors on the adjacent layers have significant dipolar couplings with different values $D_3 > D_4$ because of the buckling of the layers. Looking at Table I, we can anticipate that the boron sites close to the impurity both in the layer of the impurity and in the two adjacent layers will have internal fields large enough to give rise to additional peaks.

The absolute value of A_j is by far the largest for the nearest neighbor ($j = 1$). The value of $B_{\rm int}$ for the B sites in the layer of the impurity should, therefore, be primarily determined by $\langle S_c \rangle$ of the nearest neighbor Cu site. We then conclude that B_1 and B_2, which show large negative $B_{\rm int}$ (~ -0.14 T, see Fig. 1), must correspond to the boron sites next to either Cu_A or Cu_C in Fig. 2. Likewise, B_{15}, with its large positive $B_{\rm int}$ ($\sim$0.07 T), should be next to Cu_B. The values of $\langle S_c^A \rangle$ and $\langle S_c^C \rangle$ can be estimated approximately as $B_{\rm int}/A_1 \sim 0.2$, which is significantly smaller than the saturated value of 0.5. Thus, the distribution of $B_{\rm int}$ provides a direct experimental proof for the polaronic spin structure near defects.

Interestingly, the integrated intensity of the low frequency satellite line of B_1 at 87.12 MHz is twice as large as that of B_2 at 87.24 MHz. Since each Zn impurity creates one Cu_A and two Cu_C sites, B_1 (B_2) must be assigned to boron sites next to Cu_C (Cu_A). The larger value of $|B_{\rm int}|$ at B_1 then leads us to conclude that $\langle S_c^A \rangle < \langle S_c^C \rangle$. Figure 3(c) shows that this condition is met only in a very narrow range of α between 0.655 and 0.68.

Thanks to this assignment, we are now in a position to fix α and T_1 by fitting the experimental value of $B_{\rm int}$ at the B_1 and B_2 sites using the 36-site cluster results (interpolated between $\alpha = 0.66$ and 0.67). This leads to $\alpha = 0.665$ and $T_1 = -0.563$ T ($A_1 = -0.724$, $A_2 = -0.009$ T), compatible with the values in Table I. The full theoretical histogram of $B_{\rm int}$ deduced from Eq. (2) is plotted in the upper panels of Figs. 4(a) and 4(b). The isolated red lines in Fig. 4(a) represent $B_{\rm int}$ at the boron sites in the same layer as the impurity. Each of them is nearest to one of the seven Cu sites (Cu_{A-G}) carrying appreciable magnetization. The overall agreement between the ED results and experiment is very good, leading to the assignment of the lines B_3, B_4, B_{13}, B_{14}, and B_{15} (see Fig. 2).

Since other boron sites in the layer of the impurity have much smaller internal fields, we now turn to the neighboring layers. They have smaller values of $B_{\rm int}$ coming from the interlayer dipolar couplings D_3 or D_4 as shown in the upper panel of Fig. 4(b). Again, the agreement with the experimental results is very good. Let us focus on the experimental lines B_{11} and B_{12}. Since B_{12} is twice as intense as B_{11} (see Fig. 1), we must assign B_{12} to the neighbors of Cu_C in the layer above, and B_{11} to the neighbor of the Cu_A in the layer below. Since both couplings are given by D_3, the larger $B_{\rm int}$ at B_{12} than B_{11} provides an independent

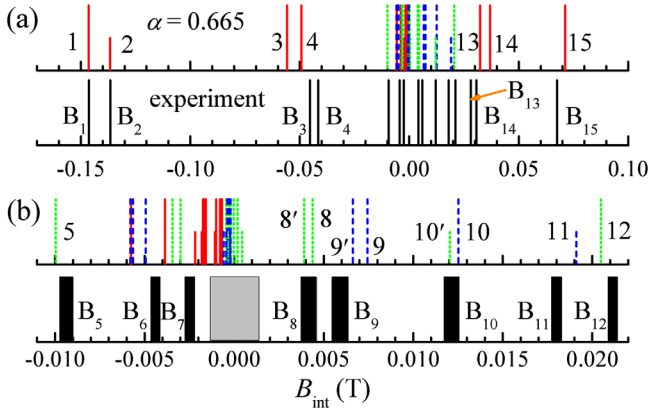

FIG. 4 (color online). (a) $B_{\rm int}$ at the B sites calculated by using the spin density distribution with $\alpha = 0.665$ for 36 sites (upper panel) and $B_{\rm int}$ deduced from experiment (lower panel). The data near $B_{\rm int} = 0$ T are expanded in Fig. 4(b). The thickness of the lines in the lower panel indicates the half width at the half maximum of the corresponding peaks of the NMR spectrum. In the calculated histograms, red solid lines correspond to B sites in the layer of the Zn impurity, green dotted (blue dashed) lines to B in the adjacent layer above (below) the impurity, and the height is proportional to the number of B sites having exactly the same internal field (1 or 2).

confirmation that $\langle S_c^A \rangle < \langle S_c^C \rangle$. With its strongly negative $B_{\rm int}$, the line B_5 must be attributed to the neighbors of Cu_B in the layer above. Discussion on the other lines is given in the Supplemental Material *E* [28].

So far, we have assumed that the hyperfine couplings are not influenced by Zn-doping. However, the small difference in the ionic radii between Cu^{2+} and Zn^{2+} (about 5% [33]) could produce nonuniform chemical pressure effects, which may result into a local lattice distortion and a modification of the hyperfine couplings. To estimate such effects, the quadrupole splitting ν_Q is a useful probe since it is sensitive to changes in local structure and charge density. The inset (b) of Fig. 3 shows the values of ν_Q for all the observed B NMR lines. Remarkably, most sites have exactly the same value $\nu_Q = 1.25$ MHz as in undoped $SrCu_2(BO_3)_2$ (solid line). Only the lines B_{11} and B_{15} show minor deviations of about 0.02 MHz, indicating that the effects of lattice distortion are small and limited to the immediate vicinity of the Zn impurities. Note that ν_Q at the boron sites close to Cu_A and Cu_C is unchanged, an indication that the hyperfine couplings are likely to remain the same. Furthermore, the dipolar coupling, which varies slowly with distance as $1/r^3$, should not be affected by a small lattice distortion. Therefore, our conclusion $\langle S_c^A \rangle < \langle S_c^C \rangle$ should remain valid even allowing for a local distortion around the impurity.

Finally, let us compare the values of α reported so far from various measurements. The analysis of susceptibility and specific heat data of the undoped material by the Shastry-Sutherland model with an interlayer coupling has led to the best value $\alpha = 0.635$ [24], while the recent determination of the width of the 1/2 plateau in very high magnetic fields up to 118 T [23] led to $\alpha \simeq 0.63$. These values are smaller than our estimate $\alpha = 0.665$ necessary to account for the internal structure of the polaron. After discarding other possibilities such as Dzyaloshinsky-Moriya (we checked with ED for the Zn -doped system that neither the intradimer nor the interdimer Dzyaloshinsky-Moriya coupling was able to account for the discrepancy), we came to the conclusion that the most likely explanation is that the ratio α increases near Zn due to the local chemical pressure induced by the larger ionic radius of Zn^{2+} as compared to Cu^{2+}. Indeed, a similar effect has already been observed in undoped samples under hydrostatic pressure [34]. To actually demonstrate that this local modification could explain the discrepancy, we have examined a simple model in which the Cu-Cu bond closest to Zn; i.e., the Cu_A-Cu_B bond $J_{\rm imp}$ is allowed to change from the bulk J' (see Supplemental Material *F* [28]). We found that the polaronic structure derived from NMR is actually compatible with $\alpha \simeq 0.65$ if $J_{\rm imp}$ is allowed to take larger values in the range 0.72–0.77. This value of α is already significantly lower than the estimate 0.665 for the uniform system, and it sounds plausible that this value can be further lowered if one allows for additional modifications of the coupling constants. It would be interesting to investigate this possibility further with the help of *ab initio* investigations of the local exchange couplings of Zn-doped. This however goes far beyond the scope of the present Letter.

We acknowledge useful discussions with C. Berthier and M. Horvatić. This work was supported by Japan Society for the Promotion of Science (JSPS) KAKENHI (B) (Grant No. 21340093), the MEXT-GCOE program, and the Swiss National Foundation. Numerical simulations were performed at CALMIP and GENCI.

[1] H. Alloul, J. Bobroff, M. Gabay, and P. J. Hirschfeld, Rev. Mod. Phys. **81**, 45 (2009).
[2] M. Hagiwara, K. Katsumata, I. Affleck, B. I. Halperin, and J. P. Renard, Phys. Rev. Lett. **65**, 3181 (1990).
[3] S. H. Glarum, S. Geschwind, K. M. Lee, M. L. Kaplan, and J. Michel, Phys. Rev. Lett. **67**, 1614 (1991).
[4] M. Yoshida, K. Shiraki, S. Okubo, H. Ohta, T. Ito, H. Takagi, M. Kaburagi, and Y. Ajiro, Phys. Rev. Lett. **95**, 117202 (2005).
[5] F. Tedoldi, R. Santachiara, and M. Horvatić, Phys. Rev. Lett. **83**, 412 (1999).
[6] J. Das, A. V. Mahajan, J. Bobroff, H. Alloul, F. Alet, and E. S. Sørensen, Phys. Rev. B **69**, 144404 (2004).
[7] M. Takigawa, N. Motoyama, H. Eisaki, and S. Uchida, Phys. Rev. B **55**, 14129 (1997).
[8] K. Kudo, T. Noji, Y. Koike, T. Nishizaki, and N. Kobayashi, J. Phys. Soc. Jpn. **73**, 3497 (2004).

[9] S. El Shawish and J. Bonča, Phys. Rev. B **74**, 174420 (2006).
[10] S. Haravifard, S. R. Dunsiger, S. El Shawish, B. D. Gaulin, H. A. Dabkowska, M. T. F. Telling, T. G. Perring, and J. Bonča, Phys. Rev. Lett. **97**, 247206 (2006).
[11] S. Capponi, D. Poilblanc, and F. Mila, Phys. Rev. B **80**, 094407 (2009).
[12] B. S. Shastry and B. Sutherland, Physica (Amsterdam) **108B+C**, 1069 (1981).
[13] H. Kageyama, K. Yoshimura, R. Stern, N. V. Mushnikov, K. Onizuka, M. Kato, K. Kosuge, C. P. Slichter, T. Goto, and Y. Ueda, Phys. Rev. Lett. **82**, 3168 (1999).
[14] K. Kodama, J. Yamazaki, M. Takigawa, H. Kageyama, K. Onizuka, and Y. Ueda, J. Phys. Condens. Matter **14**, L319 (2002).
[15] S. Miyahara and K. Ueda, Phys. Rev. Lett. **82**, 3701 (1999).
[16] A. Koga and N. Kawakami, Phys. Rev. Lett. **84**, 4461 (2000).
[17] P. Corboz and F. Mila, Phys. Rev. B **87**, 115144 (2013).
[18] K. Onizuka, H. Kageyama, Y. Narumi, K. Kindo, Y. Ueda, and T. Goto, J. Phys. Soc. Jpn. **69**, 1016 (2000).
[19] K. Kodama, M. Takigawa, M. Horvatić, C. Berthier, H. Kageyama, Y. Ueda, S. Miyahara, F. Becca, and F. Mila, Science **298**, 395 (2002).
[20] S. E. Sebastian, N. Harrison, P. Sengupta, C. D. Batista, S. Francoual, E. Palm, T. Murphy, N. Marcano, H. A. Dabkowska, and B. D. Gaulin, Proc. Natl. Acad. Sci. U.S.A. **105**, 20157 (2008).
[21] M. Jaime, R. Daou, S. A. Crooker, F. Weickert, A. Uchida, A. E. Feiguin, C. D. Batista, H. A. Dabkowska, and B. D. Gaulin, Proc. Natl. Acad. Sci. U.S.A. **109**, 12404 (2012).
[22] M. Takigawa, M. Horvatić, T. Waki, S. Kramer, C. Berthier, F. Levy-Bertrand, I. Sheikin, H. Kageyama, Y. Ueda, and F. Mila, Phys. Rev. Lett. **110**, 067210 (2013).
[23] Y. H. Matsuda, N. Abe, S. Takeyama, H. Kageyama, P. Corboz, A. Honecker, S. R. Manmana, G. R. Foltin, K. P. Schmidt, and F. Mila, Phys. Rev. Lett. **111**, 137204 (2013).
[24] For an early review, see S. Miyahara and K. Ueda, J. Phys. Condens. Matter **15**, R327 (2003).
[25] For a recent review, see M. Takigawa and F. Mila, in *Introduction to Frustrated Magnetism*, edited by C. Lacroix, P. Mendels, and F. Mila (Springer, New York, 2011), p. 241.
[26] H. Kageyama, K. Onizuka, T. Yamauchi, and Y. Ueda, J. Cryst. Growth **206**, 65 (1999).
[27] K. Kudo, T. Noji, Y. Koike, T. Nishizaki, and N. Kobayashi, J. Phys. Soc. Jpn. **70**, 1448 (2001).
[28] See the Supplemental Material at http://link.aps.org/supplemental/10.1103/PhysRevLett.114.056402, which includes Refs. [26,29–31], for details about the experiments and the theory.
[29] A. Abragam, *The Principles of Nuclear Magnetism* (Oxford University Press, London, 1961).
[30] M. Takigawa and G. Saito, J. Phys. Soc. Jpn. **55**, 1233 (1986).
[31] C. H. Recchia, K. Gorny, and C. H. Pennington, Phys. Rev. B **54**, 4207 (1996).
[32] A. Läuchli, S. Wessel, and M. Sigrist, Phys. Rev. B **66**, 014401 (2002).
[33] R. D. Shannon, Acta Crystallogr. Sect. A **32**, 751 (1976).
[34] M. E. Zayed, Ph.D. thesis, EPFL, 2010; M. E. Zayed, Ch. Rüegg, E. Pomjakushina, M. Stingaciu, K. Conder, M. Hanfland, M. Merlini, and H. M. Ronnow, Solid State Commun. **186**, 13 (2014).